Catalytic Oxidation of Hydrogen Chloride in a Fluid Bed Reactor

The Deacon reaction ($HCl + 1/4\ O_2 \rightleftharpoons 1/2\ Cl_2 + 1/2\ H_2O$) was studied in a catalytic fluid bed reactor. Reaction rates found from measurements in differential and integral reactors were represented by the Langmuir-Hinshelwood type rate equation. Considering the effect of catalysts in the dilute phase, it was found that conversions in a fluid bed reactor can be calculated without any modifying parameters. It is pointed out that the wake fraction, which has been necessary to consider for fast reactions in a fluid bed reactor, is attributed to the dilute phase effect.

SHINTARO FURUSAKI

Mitsui Toatsu Chemicals, Inc.
Yokohama-shi, Japan 247

SCOPE

Many investigators have analyzed fluid bed catalytic reactors. It is well known that the bed consists of the dense phase where most of catalysts exist and of the dilute phase. It is also known that the dense phase consists of both the bypassing bubble phase and the emulsion phase. Mass transfer between these two phases is the important factor which influences the conversion of a catalytic fluid bed reactor. This mass transfer rate is strongly affected by bubbling characteristics, and many investigations have been carried out to describe the character and size of the bubbles. Kunii (1966) states that the mass transfer resistance in the dense phase exists first between bubbles and the surrounding cloud and second between the cloud and emulsion. Both resistances are in series, and the reaction in the cloud and wake, which are the catalyst-containing-part in the bubble phase, is important for fast reactions. It has been reported that the association and growing of bubbles were important (Shichi et al., 1968; Toei et al., 1969; Mori and Muchi, 1970). Miyauchi and Morooka (1969) analyzed the mass transfer by the concept of simultaneous reaction and mass transfer. They proposed the chemical reaction factor (Hatta No.) to apply to this mass transfer.

Reaction data in the fluid bed have also been reported by many investigators. But most data are not suitable for the study of the reactor design because conversions in these studies were controlled only by the reaction rate, and mass transfer did not play an important role. Industrially, fluid beds are operated at a large linear velocity, and in this case, a large amount of catalyst is observed in the dilute phase. It is not reasonable to neglect the dilute phase. Many models of the analysis of fluid bed reactors have been presented (Kobayashi and Arai, 1965; Kato and Wen, 1969; Kunii and Levenspiel, 1969; Mori and Muchi, 1970), but these have dealt only with the character of the dense phase. It has been shown recently by Miyauchi (1973) that the contribution of the cloud and wake in the bubbling bed model (Kunii and Levenspiel, 1968) may be interpreted as the effect of catalyst particles suspended in the dilute phase. This approach has the particular advantage that the fraction of catalyst f_w (which contacts with bubble-phase gas) need not be assumed. Instead of introducing f_w, the new model can predict the extent of reaction from the quantity of catalyst in the dilute phase.

This paper presents an analysis on the fluid bed catalysis of the Deacon reaction. The reaction was carried out with a large linear velocity and under the condition of high reaction rates. Mass transfer is calculated by the theory of Miyauchi and Morooka (1969). Conversions are correlated with measured bubble diameters. First, a conventional analysis is made. Then, the importance of the effect of the dilute phase is studied. Finally reaction data of the hydrogenation of ethylene (Lewis et al., 1959) are also compared.

CONCLUSIONS AND SIGNIFICANCE

In this paper, reaction data of the Deacon reaction in a 5.5-cm diameter fluid bed reactor have been analyzed. Reaction rates are presented by the Langmuir-Hinshelwood type equation. Conversions in the fluid bed are analyzed with data of bubble size measurements, adsorption equilibria, and catalyst fractions in the dilute phase. When catalysts in the dilute phase are considered, as presented by Miyauchi (1973), the results in the fluid bed reactor can be explained without any parameters. The role of the catalysts in the bubble phase, which has been used in conventional analyses, may be attributed to the existence of catalysts in the dilute phase, especially for large linear velocity. The series combination model of the dense and dilute phases is described as another approach for analyzing results in a fluid bed.

EXPERIMENT

Catalytic oxidation of hydrogen chloride into chlorine is industrially important because of a large amount of byproduct HCl and shortage of chlorine in petrochemical industry. The Deacon reaction was chosen as a model reaction to study the characteristics of a fluid bed for the following reasons. That is, the reaction proceeds only in the presence of the catalyst. The heat of the reaction is rather small. The reaction rate is expressed by the Langmuir-Hinshelwood type equation.

S. Furusaki is with the Department of Chemical Engineering, University of Tokyo, Tokyo, Japan.

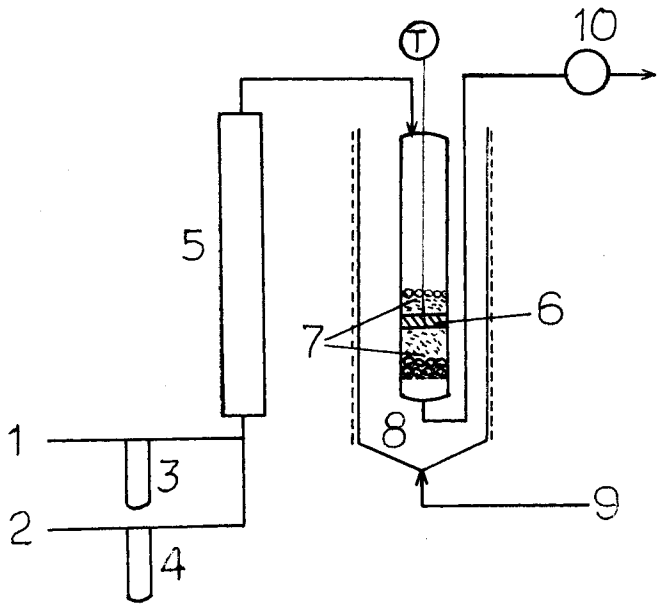

Fig. 1. Apparatus for reaction rate measurements: 1. Air compressor; 2. HCl bomb; 3, 4. Orifice; 5. SiO_2 gel dehumidiator; 6. Catalyst bed; 7. Glass beads; 8. Fluidized sand bath; 9. Air; 10. Gas flow meter; T. Thermocouple.

TABLE 1. PHYSICAL CONSTANTS OF THE CATALYST

Catalyst surface	542 m^2/g
Pore volume	0.85 ml/g
Average diameter	84 micron
Skeltal density	2.26 g/cm^3
Minimum fluidization velocity	0.6 cm/sec

TABLE 2. REACTION RATE CONSTANT OF THE DEACON REACTION

$$k = 126 \exp(-9850/RT)$$
$$K_1 = 0.0651 \exp(3430/RT)$$
$$K_2 = 0.333 \times 10^{-7} \exp(24700/RT)$$

The catalyst used is the mixture of $CuCl_2$ (11.9%), KCl (4.3%), and $SnCl_2$ (5.5%) prepared on MS silica carrier. The activity of the catalyst was stable and almost constant for a 200-hr. continuous run from catalyst life test data. The reaction scheme is as follows:

$$HCl + 1/4O_2 \rightleftharpoons \tfrac{1}{2} Cl_2 + \tfrac{1}{2} H_2O \qquad (1)$$

The heat of reaction of Equation (1) is $\Delta H = -6.95$ kcal at 600°K. Physical constants of the catalyst are shown in Table 1.

Reactor Rate

Reaction rates were measured both by the differential and by the integral reactor. The apparatus is shown in Figure 1. The diameter of the reactor was 23 mm (that of thermometer, 6 mm) with 0.5g of catalyst (2 mm bed height) when it was used as a differential reactor. As an integral reactor the diameter was 12.1 mm (effective cross-sectional area, 1.15 cm^2) with $0.5 \sim 2$g of catalyst. In the integral reactor, catalysts were mixed with glass beads (0.1 mm diameter) to make the bed height about 3 cm. Conversions were obtained by titration of Cl_2 and HCl dissolved in KI solution and NaOH solution, respectively.

Differential Reactor Analysis

Initial reaction rates were obtained from results in the differential reactor by Equation (2).

$$F(\Delta c) = \text{Rate} \cdot W \qquad (2)$$

Conversion data over 15% were omitted from the calculation. In Figure 2 are shown the experimental values of the initial rate obtained from the results in the differential reactor. A rate equation (3) was proposed from several preliminary calculations by the Langmuir-Hinshelwood approach. From the initial rates of Figure 2, the values k and K_1 in Equation (3) were obtained by multiple linear regression considering c_{Cl_2} as zero. The calculated value using the rate Equation (3) is shown by the solid lines in order to compare with the experiments.

$$\text{Rate} = \frac{k(c_{HCl}\, c_{O_2}^{1/4} - (1/K_c)\, c_{Cl_2}^{1/2}\, c_{H_2O}^{1/2})}{(1 + K_1 c_{HCl} + K_2 c_{Cl_2})^2} \qquad (3)$$

where K_c is the equilibrium constant of the reaction calculated by Equation (4) (Arnold and Kobe, 1952).

$$\log_{10} K_p = 5881.7/T - 0.93035 \log_{10} T + 1.37014 \times 10^{-4} T - 1.7581 \times 10^{-8} T^2 - 4.1744 \qquad (4)$$

Integral Reactor Analysis

Conversions obtained by the integral reactor are shown in Figure 3. Differentiating this with regard to W/F, the reaction rate can be obtained. From this reaction rate, the value of K_2 was obtained. The final values of k, K_1, and K_2 are correlated with the temperature as shown in Table 2.

The unit of c and Rate in Equation (3) are mg-mol/l and mg-mol HCl/g-cat s, respectively.

The values of the rate constants calculated by simple (unweighted) nonlinear estimation with respect to the logarithm of the reaction rate gave similar results, but the values in Table 2 will be used for later calculations. The calculated values using the constants shown above are represented by solid lines in Figure 3. Coincidence with the experimental values is quite satisfactory.

Adsorption Equilibria

Adsorption equilibrium is necessary to calculate Equation (12) with regard to the volumetric effect (Miyauchi, 1965) in the reactor. Measurements were carried out according to

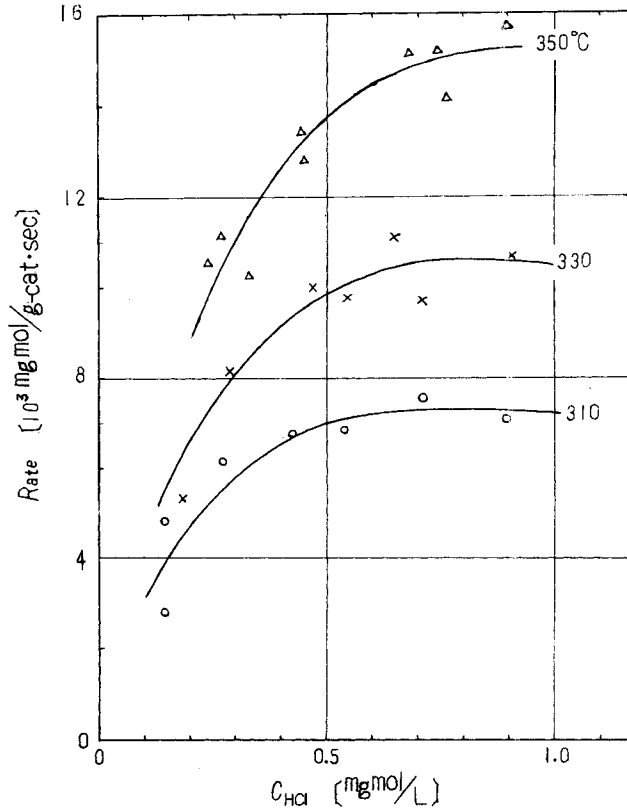

Fig. 2. Initial reaction rate.

the method of Morooka and Miyauchi (1969). The weighted catalyst was packed in a gas chromatographic tube which was heated to the reaction temperature. N_2 gas was passed through the tube. Into the stream of the carrier gas of N_2, an impulse of a tracer gas was added. The concentration of the output gas was recorded by means of a thermal conductivity cell. The value of the adsorption equilibrium constant m was calculated from the difference of the retention volume for the sample and for the standard tracer He. It was about 5.0 $\left(\frac{\text{mg-mol}}{\text{cc-cat}} \Big/ \frac{\text{mg-mol}}{\text{cc-gas}}\right)$ for Cl_2 and 0.6 for H_20, HCl, and O_2. Temperature dependence of m was neglected.

Reaction in a Fluid Bed

Apparatus. Figure 4 shows a schematic diagram of the fluid bed oxidation system. Reactor is made of stainless steel, 55 mm-diameter, and 120 cm high. Distribution of gases at the bottom of the reactor is accomplished by a plate of sintered stainless steel of which average opening diameter is 70 microns and by glass beads of 3 mm diameter beneath the sintered plate.

Reaction. Experiments were carried out in temperatures of 310 ~ 370°C, u_0 of 20 ~ 60 cm/s, and L_c of 10 ~ 60 cm (W of 115 ~ 690 g). Chlorine in the off gas from the reactor was absorbed by KI solution and it liberated I_2, which was titrated by $Na_2S_2O_3$ solution. HCl was also absorbed partially by KI solution but mostly by NaOH solution, and the quantity was measured by the usual acid-base titration. Almost all of Cl_2 and HCl were absorbed by the solutions, and the chlorine balance of the reactor system was obtained within 5% difference. The data of bed expansion were obtained by static pressure measurements at the reaction conditions. Bed heights thus obtained were used in later calculations. Reaction data for L_c of 20 cm (W of 230 g) are shown in Figure 5. As is clear from the figure, conversions become lower with higher superficial velocity. Solid lines in the figure show conversions calculated by apparent $K_{ob}a_b$ of Figure 9, which will be explained later. Conversions in the fluid bed are compared in Figure 6 with the ones in the packed bed of Figure 3 where piston flow of gas is assumed. As is clear from the figure, conversions in the fluid bed are lower than those in the packed bed because of bypassing in the bubble phase. Also it is seen that the values of the conversions are very close for small W/F, in which case better contact is expected.

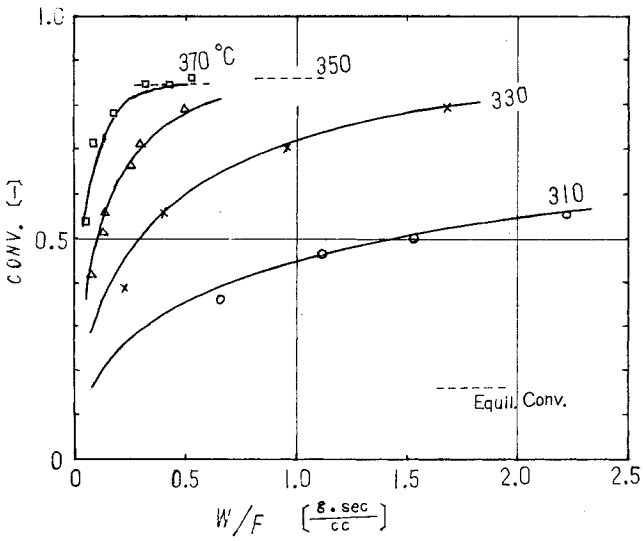

Fig. 3. Integral reactor analysis.

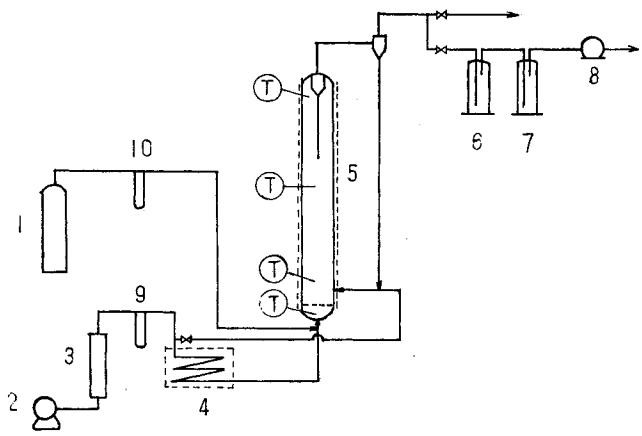

Fig. 4. Fluid bed reactor system: 1. HCl bomb; 2. Air compressor; 3. SiO_2 gel dehumidiator; 4. Heater; 5. Fluid bed reactor; 6. Cl_2 absorber (KI soln.); 7. HCl absorber (NaOH soln.); 8. Gas flow meter; 9, 10. Orifice; T. Thermocouple.

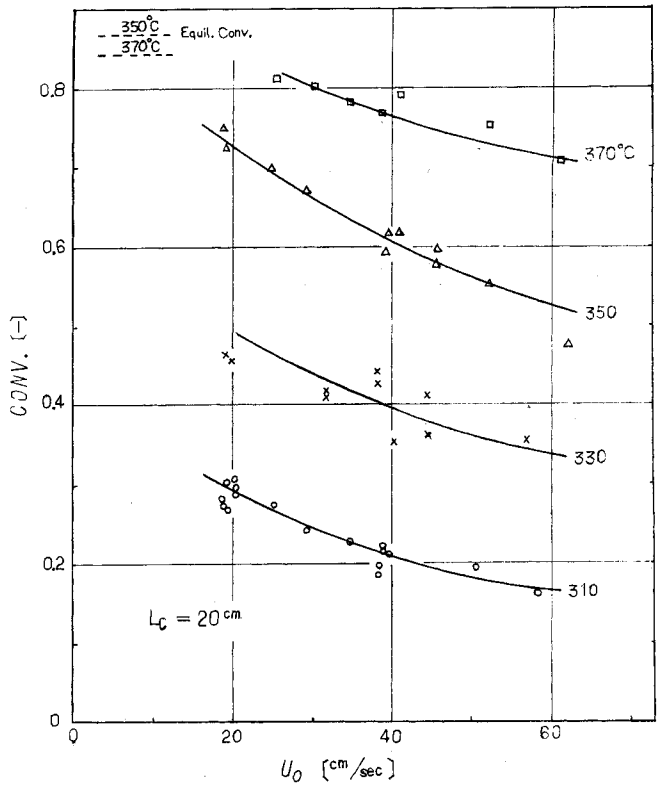

Fig. 5. Fluid bed reaction data for L_c = 20 cm.

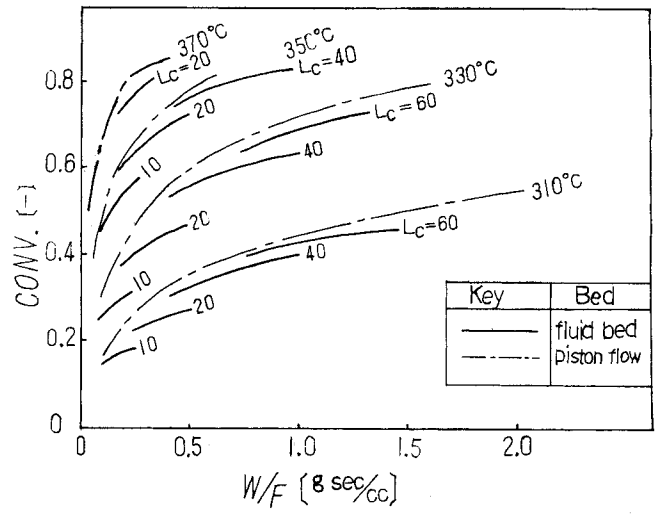

Fig. 6. Comparison of the fluid bed reactor to a piston flow reactor.

Bubble Size

Bubble sizes were measured according to Kunii and Levenspiel's method (1968). Bubble diameters were obtained by bubble frequency measurements. They are shown with regard to superficial velocities (Figure 7).

EXAMINATION OF THE REACTION DATA NEGLECTING THE DILUTE PHASE

A gas-phase fluid bed reactor is considered to be a heterogeneous reactor which comprises the bubble phase and the emulsion phase. In analyzing the reactor, gas flow in the bubble phase is considered to be piston flow as usual. The mixing in the emulsion phase is not important in ordinary cases (Furusaki, 1968) and the longitudinal dispersion in the emulsion phase is neglected for later analysis. Gas flow in the emulsion phase is also neglected because almost all of the gas passes through the bubble phase in a fluid bed, where superficial velocity u_0 is about

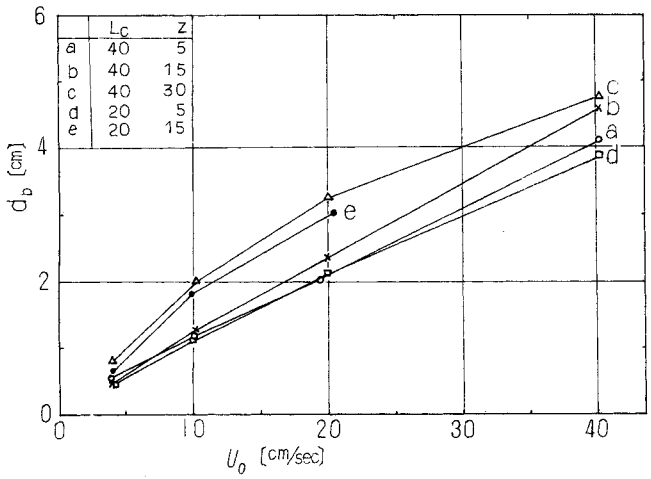

Fig. 7. Bubble size measurement.

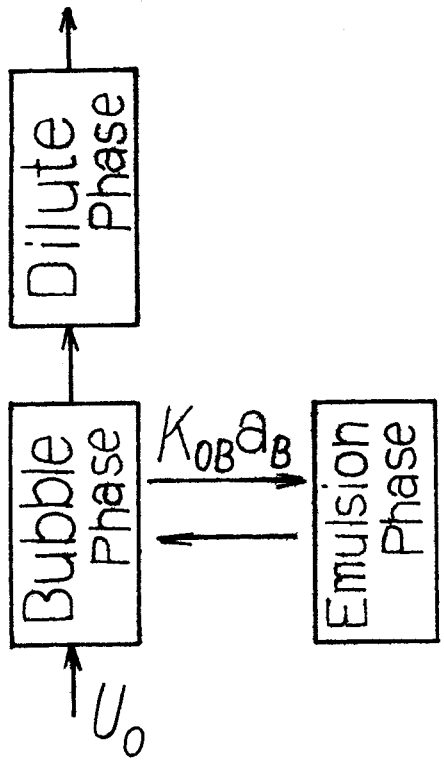

Fig. 8. Model for a fluid bed reactor.

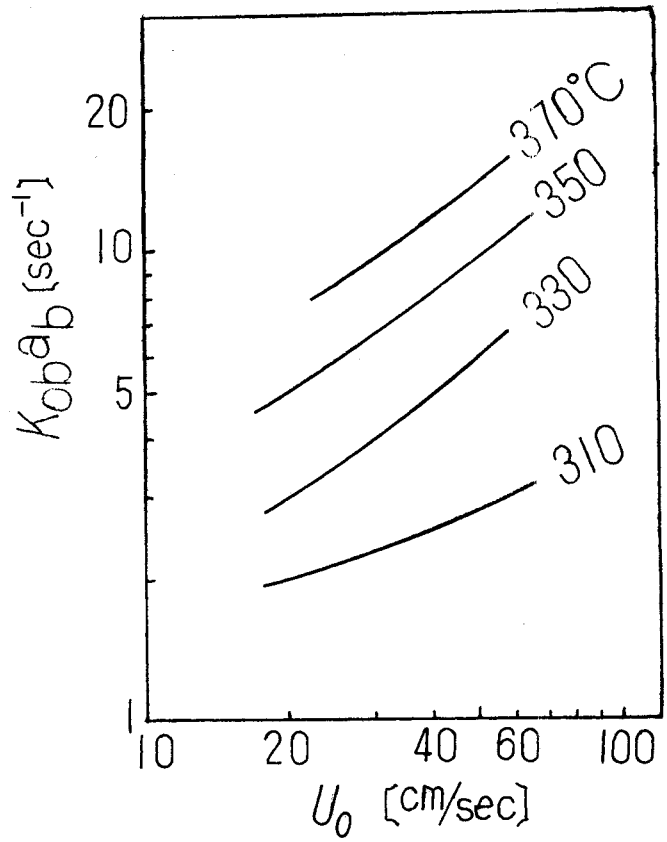

Fig. 9. Apparent $K_{ob}a_b$ with $f_w = 0$.

50 ~ 100 times greater than u_{mf}. [Superficial gas velocity in the emulsion phase is considered to be u_{mf}, and in the bubble phase, $u_0 - u_{mf}$, according to Davidson and Harrison (1963)].

Figure 8 shows flow of materials in a fluid bed reactor. Material balances of reactants and products between the height $z \sim z + dz$ for both bubble and emulsion phase give the following equations:

$$u_0 \frac{dc_i^b}{dz} + K_{0bi}a_b(c_i^b - c_i^e) + \alpha\epsilon_e\rho_{mf}(\nu_i \,\mathrm{Rate}(c_i^b)) = 0 \tag{5}$$

$$K_{0bi}a_b(c_i^b - c_i^e) - (1-\alpha)\rho_e(\nu_i \,\mathrm{Rate}(c_i^e)) = 0 \tag{6}$$

$$\alpha = f_w\epsilon_b/\epsilon_e \tag{7}$$

$$\rho_e = W/AL_f \tag{8}$$

The boundary condition at $z = 0$ is

$$c_i^b = c_i^0 \tag{9}$$

where rate (c_i^b) and rate (c_i^e) mean that the reaction rate is to be calculated with concentration in the bubble and the emulsion phases, respectively.

According to Miyauchi and Morooka (1969) mass transfer between the bubble and emulsion in a fluid bed is to be treated as so-called "simultaneous" mass transfer and reaction. Davidson and Harrison (1963) showed the velocity of a single bubble relative to the emulsion as $0.711\sqrt{gd_b}$. Applying Higbie's penetration theory and putting $\tau = d_b/u_b$,

$$K_{0bi} = \frac{\beta_i k_{bi} k_{ei}}{k_{bi} + \beta_i k_{ei}} \tag{10}$$

$$k_{bi} = 2\sqrt{\frac{D_i}{\pi\tau}} \tag{11}$$

$$k_{ei} = 2\sqrt{\epsilon_{mf}(\epsilon_{mf} + m_i(1 - \epsilon_{mf}))D_i/\pi\tau} \qquad (12)$$

β_i is the reaction factor (Hatta number). Here, voids of the emulsion phase are assumed to be the same as that of the incipient fluidization. The mass transfer surface a_b is given by 6 ϵ_b/d_b where $\epsilon_b = (u_0 - u_{mf})/(u_0 - u_{mf} + 0.711\sqrt{gd_b})$. It is also assumed that the gas bubble rises at a velocity of $u_0 - u_{mf} + 0.711\sqrt{gd_b}$ according to Davidson and Harrison (1963).

If catalysts are neglected in the bubble phase as the first trial, average values of $K_{0b}a_b$ for reactants and products are obtained from the conversions by computational simulations of Equation (5) to (9) by taking $\alpha = 0$. These

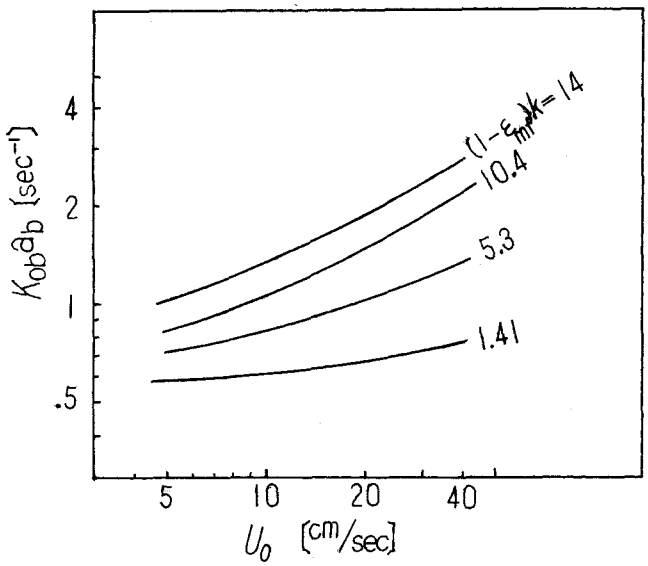

Fig. 10. Apparent $K_{0b}a_b$ from the data of Lewis et al. (1959).

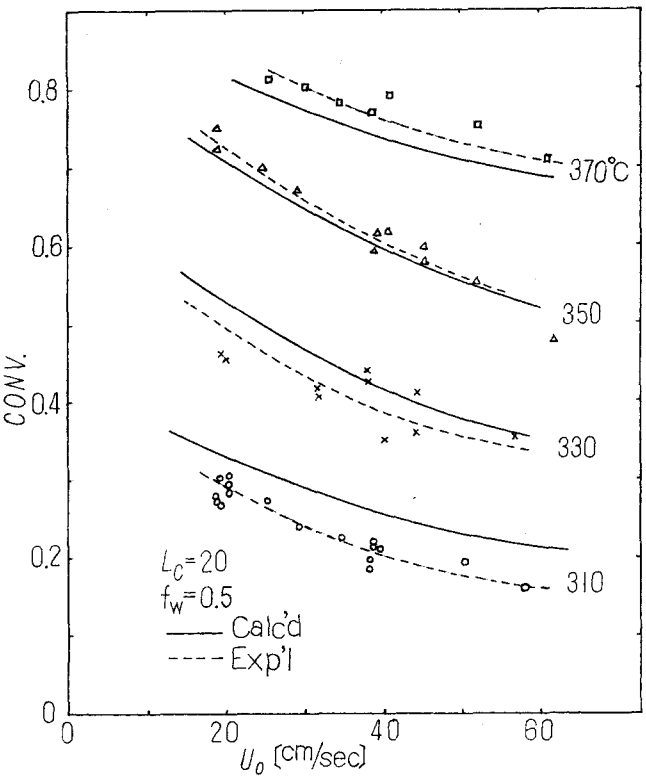

Fig. 11. Conversions calculated with d_b measured by Kunii and Levenspiel's method, $f_w = 0.5$.

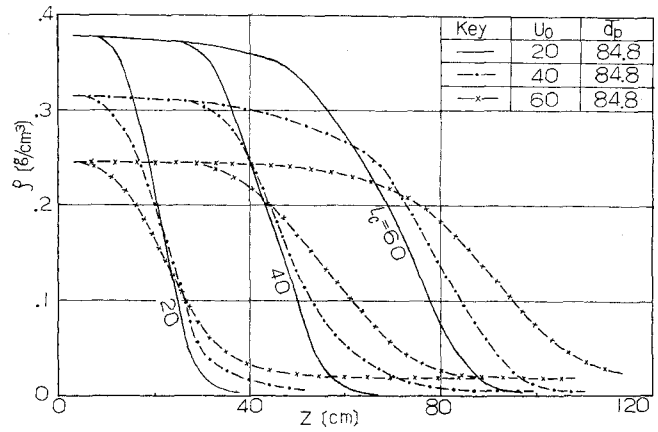

Fig. 12. Bed density (Miyauchi, 1973).

are shown in Figure 9. Integration of the equations is done between z = 0 and $z = L_f$ where L_f is obtained by measuring the bed density. $K_{0b}a_b$ did not change significantly with the bed height for $L_c \geq 20$ cm. Similar calculations for the data of Lewis et al. (1959) are shown in Figure 10 for comparison. Their data cover the catalyst activities between 1.1 and 14.3 s^{-1}. $K_{0b}a_b$ is found to be a strong function of temperature, that is, a function of the rate of the reaction for both cases. But $K_{0b}a_b$ should not change significantly with the temperature or rate of reaction because the bubble size is not affected by them.

To solve the discrepancy, one must consider the existence of catalyst particles in the bubble phase. Davidson and Harrison (1963) have shown the thickness of the cloud as $\left(\left(\frac{u_b\epsilon_{mf}/u_{mf} + 2}{u_b\epsilon_{mf}/u_{mf} - 1}\right)^{1/3} - 1\right) \times \frac{d_b}{2}$. Evaluation shows that catalysts in the cloud can be neglected in calculations of reaction. Hence, catalysts in the bubble phase are attributed only to the wake of bubbles.

If we take bubble diameters of Figure 7(b) and f_w as 0.50, good agreements with the experimental data are obtained in Figure 11. Here, solid density in the wake is assumed to be the same as that of the minimum fluidization. In the figure, the solid lines show the calculated results and the broken lines show the experimental ones. f_w seems to be small for the low reaction rate, but the slope of the curves for both calculated and experimental conversions are similar. Thus, introduction of f_w can correlate the fluid bed reaction data, as Lewis et al. (1959) have assumed, of 0.05 ~ 0.2. However, the stream lines through the bubble do not pass through the wake region (Murray, 1965; Rowe et al., 1964). It seems difficult to say that the wake is inside the bubble phase. If so, the value of f_w seems to be too large compared with physical measurements of bubbles because the value of f_w reported in the literature is less than 0.01 (Kobayashi et al., 1965).

EFFECT OF THE DILUTE PHASE

The catalysts in the dilute phase have been neglected in previous studies for the analysis of the reaction in the fluid bed. However, the existence of solid particles in the dilute phase has been reported (Kunii and Levenspiel, 1968; Miyauchi et al., 1968). The bed density of the fluid bed for the FCC catalyst of the same particle size is shown in Figure 12 (Miyauchi, 1973). In the figure, ρ's stay constant in the region from $z = 0$ for some values of z, but above those values of z they reduce gradually to 0. The former region corresponds to the dense phase and the latter to the dilute phase. Therefore, a large amount of

catalysts are suspended in the dilute phase. Accounting for these catalysts, a series model (Figure 8) of the dense phase and the dilute phase has been presented by Miyauchi (1973). The dense phase consists of the dispersed bubble phase which causes bypassing of the reacting gas and of the continuous emulsion phase where most of catalysts exist. In the dilute phase, catalysts are uniformly dispersed in the gas phase except for some slugs of catalyst group. Catalysts go up in the center and go down along the wall as in the dense phase. Solid density in the dilute phase may decrease exponentially, but in later calculations it is assumed to decrease linearly as shown in Figure 13.

According to Figure 8 the following equations will be written. For the dense phase, they are shown in Equations (5) and (6). d_b of Figure 7(b) is used for the calculations. The bed density is calculated from Equation (13) where L_e and L_d are defined in Figure 13.

$$\rho_e = \frac{2W}{A(L_e + L_d)} \tag{13}$$

For the dilute phase, neglecting the longitudinal mixing of the gas phase and adsorbed materials in the solid phase,

$$\rho_{sd} = \rho_e \frac{L_d - z}{L_d - L_e} \tag{14}$$

$$\frac{dc}{dz} = -\frac{\rho_{sd}}{u_0} \text{Rate } (c) \tag{15}$$

with the equations solved for the experimental conditions, the results are compared with the experimental data in Figure 14. The abscissae for those values of u_0 designated in the figure were obtained from the smoothed curves of the experimental results shown in Figure 5. The ordinates of the black dots in Figure 14 show the calculated conversions at the boundary of the dense and dilute phases. The total calculated conversions are designated by the points at the upper end of the dotted lines. So the length of the dotted lines shows the extent of conversions in the dilute phase. From the figure, the contribution of the dilute phase is obviously quite important. The experimental data show higher conversions than the calculated values. One reason is probably good contact of catalysts and gas at the onset of elutriation near the boundary of the dense phase and dilute phase. The existence of small amounts of catalysts ($f_w = 0.02$) did not make any significant difference (less than 5% of conversion). Examination of Figure 14 indicates good agreement of the calculated results with the experimental data considering that we assumed no arbitrary parameters in this analysis.

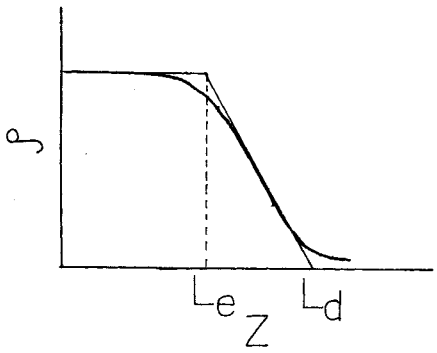

Fig. 13. Linear approximation of the bed density.

DISCUSSION

Figure 14 shows that the data of the Deacon reaction in the fluid bed, as an example of fast reaction expressed by the Langmuir-Hinshelwood type kinetics, can be calculated by the series model (Miyauchi, 1973) of the dense phase and the dilute phase. Without considering the effect of the dilute phase, one must assume catalyst particles in the bubble phase f_w to explain the results as shown before. Since the stream lines of gas flow inside the bubbles do not pass through the wake as mentioned before, this treatment of f_w is questionable, although values of f_w simulated are about comparable to those obtained by the photographic study by Rowe (1965). If one examines the significance of Figure 12, the effect of the dilute phase is quite reasonable. It is very important that fast reactions in a fluid bed are estimated from data on bubbles and on the dilute phase without any parameters such as f_w. Therefore, the solid fraction so far considered in the analyses of fluid bed reactors may be attributed to suspended solids in the dilute phase.

Lewis et al. (1959) have shown the data of the hydrogenation of ethylene in a fluid bed, and they seem to be the only data of a fast reaction so far published in the literature. Calculation of their data by the series model is shown in Figure 15 where L_e and L_d are estimated from Miyauchi's measurement (1973) for F.C.C. catalysts of the same size. Values of the gas interchange rate between

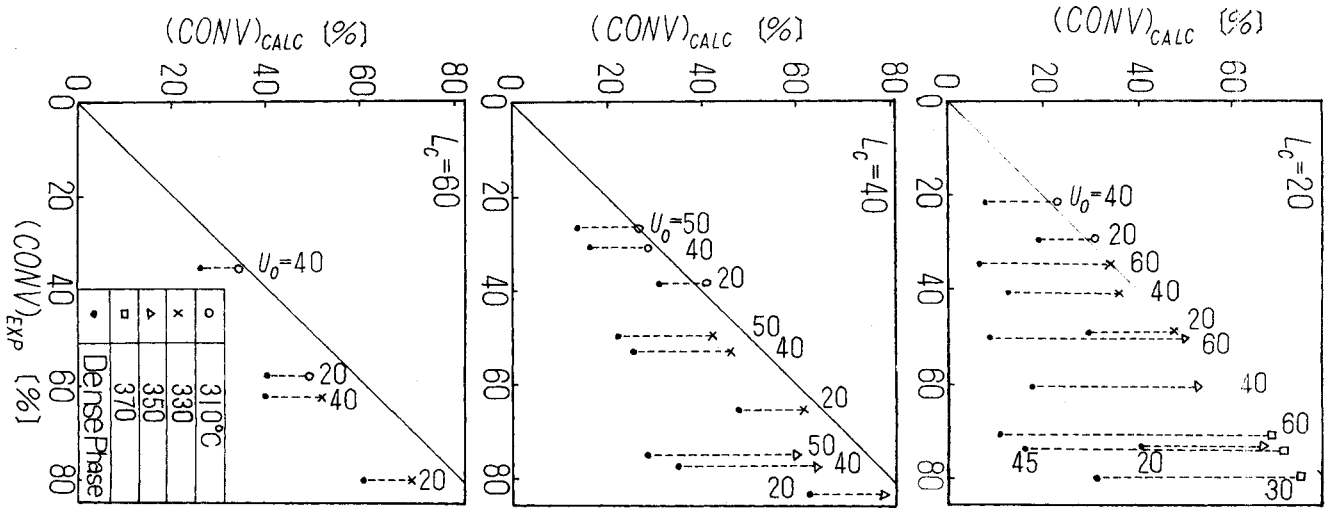

Fig. 14. Effect of the dilute phase.

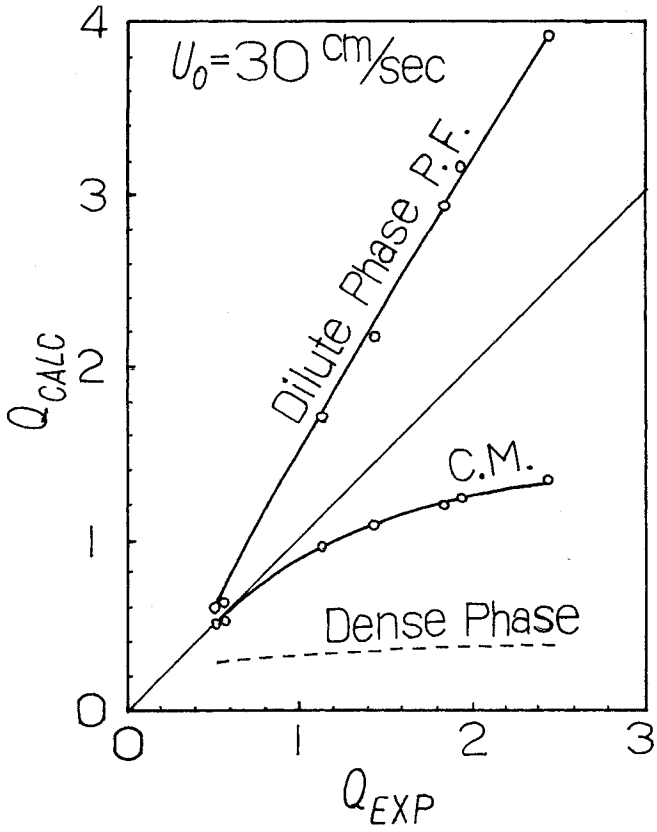

Fig. 15. Effect of the dilute phase for the data of Lewis et al. (1959).

the bubble phase and the emulsion phase are taken from the values of Lewis et al. L_{mf}, L_e, L_d are estimated to be 67.4 cm, 57 cm, 97 cm, respectively for L_c of 60 cm. Rate constants (1st order) are between 14.3 s^{-1} and 1.29 s^{-1}. The former corresponds to the largest Q, and the latter corresponds to the smallest value of Q. From the figure, the importance of the dilute phase is again pointed out. Also, the gas flow pattern in the dilute phase is found to be at about the middle of piston flow and complete mixing in this case.

For designing of fluid bed reactors, economical evaluations demand larger capacity of production. Large linear velocity inside the bed is preferred for this purpose, giving a more important contribution of the dilute phase for reaction. Moreover, better selectivity can be expected in reaction because good contact of gas and solid is expected in the dilute phase. This is especially true for endothermic and isothermal reactions. The reactions seem to occur to some extent in the dilute phase in the F.C.C. units since the density of catalyst particles is realized to reduce gradually in the dilute phase (Ikeda, 1966).

ACKNOWLEDGMENT

The author wishes to express his gratitude to T. Miyauchi of the University of Tokyo for his stimulating discussions and helpful suggestions, and to T. Taguchi of Osaka Petrochemical Industries, Ltd. for his excellent experimental work during this study. He also thanks Mitsui Toatsu Chemicals, Inc. for permission to publish this paper.

NOTATION

A = cross-sectional area of the bed, cm^2
a_b = mass transfer area between the bubble and the emulsion, cm^2/cm^3
c = concentration of reaction species, mg-mol/l
c^0 = inlet concentration, mg-mol/l
Δc = difference between the inlet concentration and the outlet concentration
D = diffusion coefficient, cm^2/s
d_b = bubble diameter, cm
F = feed rate of the inlet gas, l/s
f_w = fraction of volume of wake to that of bubble, dimensionless
K_{0b} = overall mass transfer coefficient between the bubble phase and the emulsion phase, cm/s
k_b = film mass transfer coefficient in the bubble phase, cm/s
k_e = film mass transfer coefficient in the emulsion phase, cm/s
k, K_1, K_2, K_c = constants in the rate Equation (3)
$(1-\epsilon_{mf})k$ = first-order rate constant of Lewis et al. at the minimum fluidization condition, s^{-1}
L_c = height of the static bed, cm
L_e = height of the dense phase, cm
L_d = height of the dilute phase, cm
L_f = height of the fluid bed, cm
m = adsorption equilibrium constant, $\frac{\text{mg-mol}}{\text{cc-cat}} \Big/ \frac{\text{mg-mol}}{\text{cc-gas}}$
Q = specific converting power of Lewis et al. (1959), l/s
Rate = reaction rate, mg-mol/g.cat.s
u_0 = superficial velocity of gas, cm/s
u_b = relative velocity between bubble and emulsion, cm/s
W = weight of catalyst particles, g
z = distance from the bottom of the fluid bed, cm

Greek Letters

α = fraction of particles which exist in the bubble phase, dimensionless
β = Hatta No., dimensionless
ϵ = void fraction, dimensionless
ϵ_b = volume fraction of the bubble phase, dimensionless
ϵ_e = volume fraction of the emulsion phase, dimensionless
ν = stoichiometric factor, dimensionless
ρ = density of the bed, g/cm^3

Superscripts and Subscripts

b = bubble phase
d = dilute phase
e = emulsion phase
i = i species
s = solid

LITERATURE CITED

Arnold, C. W., and K. A. Kobe, "Thermodynamics of the Deacon Process", *Chem. Eng. Progr.*, **48**, 293 (1952).

Davidson, J. F., and D. Harrison, *Fluidized Particles*, p. 69, 100, Cambridge (1963).

Furusaki, S., "A Study on the Effect of Adsorption in Fluid Bed Reactors," *Kagaku Kogaku*, **32**, 1033 (1968).

Ikeda, Y., "Fluid Bed Reactors," *Kagaku Kikai Gijutsu*, **18**, 193, Tokyo (1966).

Kato, K., and C. Y. Wen, "Bubble assemblage model for fluidized bed catalytic reactors," *Chem. Eng. Sci.*, **24**, 1351 (1969).

Kobayashi, H., and F. Arai, "Effects of Several Factors on Catalytic Reaction in a Fluidized Bed Reactor," *Kagaku Kogaku*, **29**, 885 (1965).

———., and T. Chiba, "Behavior of Bubbles in Gas Solid Fluidized Bed," 858.

Kunii, D., "Transport Phenomena and Reaction Kinetics in a Fluidized Bed," *Kagaku Kikai Gijutsu*, **18**, 161 (1966).

———., and O. Levenspiel, "Bubbling Bed Model," *Ind. Eng. Chem. Fundamentals*, **2**, 441 (1968).

———., *Fluidization Engineering*, p. 94, 180, 242, Wiley (1969).
Lewis, W. K., E. R. Gilliland, and W. Glass, "Solid-catalyzed Reaction in a Fluidized Bed," *AIChE J.*, **5**, 419 (1959).
Miyauchi, T., "Rate Processes and the Two Phase Model for a Fluid Bed," 30th Annual Meeting, Soc. Chem. Engrs., Japan, No. 6110 (1965).
———., *J. Chem. Eng. Japan*, paper submitted (1973).
———., and S. Morooka, "Mass Transfer Rate between Bubble and Emulsion Phase in Fluid Bed," *Kagaku Kogaku*, **33**, 880 (1969).
———., "Circulating Flow and its Effects on Chemical Reaction in Fluid Bed Contactor," *ibid.*, 369.
Miyauchi, T., H. Kaji, and K. Saito, "Fluid and Particle Dispersion in Fluid-bed Reactors," *J. Chem. Eng. Japan*, **1**, 72 (1968).
Mori, S., and I. Muchi, "Mathematical Model for Catalytic Reaction in Fluidized Bed," *Kagaku Kogaku*, **34**, 510 (1970).
Morooka, S., and T. Miyauchi, "Mean Residence Time of Adsorptive Tracer Gases in Solid-Fluid Contactors", *ibid.*, **33**, 569 (1969).
Murray, J., "On the Mathematics of Fluidization," *J. Fluid Mech.*, **22**, 57 (1965).
Rowe, P. N., and B. A. Partridge, "An X-ray Study of Bubbles in Fluidized Beds," *Trans. Inst. Chem. Engrs.*, **43**, T157 (1965).
———., and E. Lyall, "Cloud formation around bubbles in gas fluidized beds," *Chem. Eng. Sci.*, **19**, 973 (1964).
Shichi, R., S. Mori, and I. Muchi, "Interaction between Two Bubbles in Gaseous Fluidization," *Kagaku Kogaku*, **32**, 343 (1968).
Toei, R., R. Matsuno, K. Nishitani, H. Hayashi, and T. Iwamoto, "Gas Interchange between Bubble Phase and Continuous Phase in Gas-Solid Fluidized Bed at Coalescence," *ibid.*, **33**, 668 (1969).

Manuscript received January 17, 1973; revision received April 13 and accepted April 17, 1973.

Application of Conformational Analysis Techniques to the Prediction of Heats of Formation and Gas-Phase Thermodynamic Functions

Conformational energy calculations based on describing the deformation of chemical bonds by energy functions allow the prediction of molecular geometries, heats of formation, vibrational frequencies, and gas-phase thermodynamic functions of compounds which contain bonds or groups of bonds whose properties are transferable from molecule to molecule.

R. H. BOYD
S. M. BREITLING
and
M. MANSFIELD

Department of Chemical Engineering
University of Utah
Salt Lake City, Utah 84112

SCOPE

In quest of predicting or estimating the properties of molecules and compounds, chemists and chemical engineers have for many years taken advantage of the fact that the properties of chemical bonds or groups of chemical bonds are often independent of the particular kind of molecule in which they reside. Highly successful empirical schemes for property prediction have been based on this principle. An outstanding example is the development of bond energy or group contribution schemes which allow the heats of formation of appropriate compounds to be calculated within the accuracy of measurement. Other examples are bond moments for molecular dipole moment calculation, transferable spectroscopic force constants for the stretching, bending, and twisting of bonds that allow vibrational frequency prediction, and natural bond lengths and angles for geometry estimation. Although there are many examples of molecules where electronic effects (often called resonance,